

## Comparison of MODIS and ETA profiles of atmospheric parameters in coastal zones with radiosonde data

M. ADAMO<sup>(1)</sup>, G. DE CAROLIS<sup>(2)</sup> and S. MORELLI<sup>(3)</sup>

<sup>(1)</sup> *Dipartimento di Fisica, Università di Bari - Bari, Italy*

<sup>(2)</sup> *CNR-ISSIA, Istituto di Studi sui Sistemi Intelligenti per l'Automazione - Bari, Italy*

<sup>(3)</sup> *Dipartimento di Fisica, Università di Modena e Reggio Emilia - Modena, Italy*

(ricevuto il 26 Luglio 2007; revisionato il 10 Ottobre 2007; approvato l' 11 Ottobre 2007)

**Summary.** — The quality of atmospheric profiles gathered by the spaceborne Moderate Resolution Imaging Spectroradiometer (MODIS) sensor onboard the Terra platform and those predicted by the ETA atmospheric circulation model are assessed against corresponding radiosonde (RS) measurements. The analysis is carried out on a statistical basis taking as reference the radiosoundings collected at two coastal stations, namely Ajaccio (France) and Pratica di Mare (Italy), during the spring 2000. The examined days were characterized by smooth and slow variations of the atmospheric conditions so that a temporal lag up to about three hours between RS and MODIS profiles could be considered for comparison purposes. Both ETA predictions and MODIS retrievals compare well with RS data and their relative agreement is good. Although, as expected, the profiles of the analyzed quantities, namely temperature and moisture for both MODIS and ETA outputs and horizontal wind components predicted by ETA model, could not follow the largest fluctuations measured by RS, their averages are reproduced with a satisfactory degree of reliability. These results encourage the perspective to exploit remote measurements from the MODIS sensor of atmospheric temperature and water vapour as input to operative circulation models, such as ETA, for reliable forecasts and detailed monitoring on global scale of the atmospheric structure and dynamics.

PACS 92.60.Aa – Modeling and model calibration.

PACS 92.60.Wc – Weather analysis and prediction.

PACS 93.85.Bc – Computational methods and data processing, data acquisition and storage.

PACS 93.85.Pq – Remote sensing in exploration geophysics.

### Introduction

The compelling climate change issue has led in the last years to the urgent need of reliable knowledge and prediction of the chemical-physical parameters concerning the whole Earth atmosphere. The traditional method of measurement employed to get information about the vertical structure of the atmosphere is mainly provided by radiosonde (RS). They allow measurements of air temperature, humidity, pressure and wind vector

at different heights, up to about 30000 meters. RS data is relevant to the volume of air crossed during its ascent and is believed to be representative of a circular area up to about 200–250 km around the station location [1].

Depending on the station schedule, RS data is typically provided two or four times every day. In contrast to the relatively high temporal rate of acquisitions, the global scale coverage is however hampered not only by the obvious lack of RS stations over the oceans, seas and remote polar regions, but also by the very sparse distribution on the land. Nowadays, it is accumulating a wealth of atmospheric data on global scale as a result of the acquisitions gathered by spaceborne radiometers. In particular, the Moderate Resolution Imaging Spectroradiometer (MODIS) instruments, the first launched on 18th December 1999 onboard the Terra Platform and the second on 4th May 2002 onboard the Aqua platform, are uniquely designed to observe and monitor atmospheric parameters. Their wide spectral range, high spatial resolution, and near daily global coverage allow monitoring of atmosphere composition along its depth.

Beside the need of data about the atmosphere composition and mapping of chemical-physical parameters on global scale, accurate numerical simulation of the atmospheric physical characteristics is also an issue. Motivations rely upon the increasing necessity to get reliable weather forecasts.

The capability of satellite-borne instrumentations to gather high-resolution atmospheric data thus represents a unique opportunity to envisage assimilation schemes into numerical models, in particular for polar regions [2, 3].

Assessed remote-sensing measurements of the atmosphere on global scale in conjunction to accurate predictions of the atmospheric conditions can thus be considered a valuable base toward improved knowledge of the atmospheric circulation.

As part of a study program concerning the atmospheric circulation and ocean dynamics of the North-Western Tyrrhenian Sea on short temporal scale, in this work an inter-comparison of the atmospheric profiles gathered by the spaceborne instrument MODIS/Terra, predicted by the ETA model and collected by RS is performed. As the chief purpose was to assess the performances of MODIS retrievals with respect to high-resolution ETA predictions, RS profiles were considered as reliable reference data within their typical instrumentation errors.

We have analyzed data from two coastal RS stations: Ajaccio (41.91° N, 8.80° E), Corsica (France) and Pratica di Mare (41.65° N, 12.43° E), Italy, respectively, for the days from 29th to 31st March 2000 and from 17th to 19th April 2000. RS observations were every twelve hours at 00:00 UTC and 12:00 UTC for Ajaccio station, while every six hours starting from 00:00 UTC at Pratica di Mare station. The radiosoundings were retrieved from the archive of the University of Wyoming. Radiosounding measurements were taken using RS-80 radiosondes manufactured by Vaisala (Helsinki, Finland). Pressure, temperature, air relative humidity and wind vector data are provided at different heights with altitude-dependent spacing. During the ascent, the atmospheric parameters are sampled at increasing altitude intervals, typically ranging from about 10 m at the lowest altitudes up to about 1900 m. Finally, the following accuracies are stated by the manufacturer: pressure:  $\pm 0.5$  hPa; temperature:  $\pm 0.2$  K; humidity:  $\pm 3\%$ ; wind speed:  $\pm 0.15$  m/s; wind direction:  $\pm 2^\circ$ .

## 1. – ETA model description

The ETA model originated in Yugoslavia, at Belgrade University and the Federal Hydrometeorological Institute. Fedor Mesinger and Zavisla Janjic developed the model.

Further development has been a team effort involving numerous scientists, primarily at National Centers for Environmental Prediction (NCEP) of the US National Weather Services, where ETA is one of the mesoscale numerical weather prediction models. It includes advanced physics and is widely used for research, and numerical prediction in several countries.

The ETA model is a three-dimensional, grid-point model. It uses a rotated spherical coordinate system and a semi-staggered Arakawa E grid. The name “ETA” derives from the model’s vertical coordinate known as the “eta” or “step mountain” coordinate [4, 5], which represent a generalization of the usual sigma coordinate. However the model can perform sigma run as well. The eta coordinate is defined by the relationship

$$(1) \quad \eta = \left( \frac{p - p_T}{p_{\text{sfc}} - p_T} \right) \left[ \frac{p_{\text{ref}}(Z_{\text{sfc}}) - p_T}{p_{\text{ref}}(0) - p_T} \right],$$

where  $p$ ,  $p_T$ ,  $p_{\text{sfc}}$  are, respectively, grid-point, model top and surface pressures;  $p_{\text{ref}}$  is a suitable reference pressure depending on altitude ( $Z$ ) (*i.e.* in a polytropic atmosphere). In contrast to the sigma coordinate, this coordinate system makes the eta surfaces quasi-horizontal everywhere. The model topography (step mountain) is constructed from three-dimensional grid boxes, obtained by rounding off the silhouette values got from the Digital Elevation Model dataset at 30'' horizontal resolution. The model is able to perform hydrostatic and non-hydrostatic run.

The physical package of the model includes: the Geophysical and Fluid Dynamics Laboratory (GFDL) radiation schemes, the Betts-Miller-Janjic convective parameterization [6], an orographic form drag scheme [7], a soil model with four layers [8] and the revised Mellor-Yamada level 2.5 turbulence scheme for the planetary boundary layer [9]. Turbulent processes in the surface layer are represented by means of Monin-Obukhov similarity theory with the Paulson scheme [10] on land points and with a scheme derived from Mellor-Yamada level 2 formulation [11] on sea points. Viscous sub-layer parameterization is also present on sea points. Sea Surface Temperatures (SSTs), interpolated to the ETA model grid, are kept constant at the initial values during integration. Prognostic variables are temperature, specific humidity, horizontal components of velocity, surface pressure, cloud water and turbulent kinetic energy.

The model simulations, presented in this paper, were carried on with three nested domains in order to obtain the high horizontal resolution. The technique used is a one-way nesting. The European Centre for Medium Range Weather Forecasts (ECMWF) initialized analyses, at  $0.5^\circ \times 0.5^\circ$  horizontal resolution, provided initial and boundary conditions for the lower resolution ETA model run. Initial conditions refer to 00:00 UTC 29 March 2000 and 12:00 UTC 17 April 2000 respectively, and the simulations last 72 hours. Model outputs of the first domain were used as boundary conditions of the second grid run and this provided the boundary conditions for the finer grid run. Vertical resolution consists of 50 layers from sea surface to 25 hPa, with higher resolution near the bottom of the domain. Horizontal resolution is  $0.125 \times 0.125$  transformed degrees (about  $20 \text{ km} \times 20 \text{ km}$  as approximate distance between two mass points on the semi-staggered Arakawa E grid) for the coarse grid,  $0.05 \times 0.05$  transformed degrees (about  $7.5 \text{ km} \times 7.5 \text{ km}$ ) for the second grid and  $0.025 \times 0.025$  transformed degrees (about  $4 \text{ km} \times 4 \text{ km}$ ) for the finer grid.

The domain size of the coarse resolution run is roughly  $2100 \text{ km} \times 2200 \text{ km}$  with central point located at  $43.5^\circ \text{N}$ ,  $9.5^\circ \text{E}$ . Time step is 36 seconds; the boundary conditions were updated every 6 hours. The second grid simulation was performed with a domain size of roughly  $900 \text{ km} \times 900 \text{ km}$ , time step is 15 seconds, and the boundary conditions were

updated every 3 hours. Inner domains, larger than  $200\text{ km} \times 200\text{ km}$  including Ajaccio and Pratica di Mare stations respectively, were used for the finer grid non hydrostatic runs. Time step is 10 seconds, updating the boundary conditions every hour. Model outputs for the finer grid were extracted every hour.

## 2. – MODIS Terra profiles

The MODerate resolution Imaging Spectoradiometer on board the Terra polar-orbiting satellite (MODIS/Terra) is an imaging instrument with 36 spectral bands between  $0.645$  and  $14.235\ \mu\text{m}$  [12]. MODIS/Terra platform was launched on 18th December 1999 by the US National Aeronautics and Space Administration (NASA) within the Earth Observing System (EOS) program. Later, on 4 May 2002, NASA launched the twin instrument on Aqua platform (MODIS/Aqua).

MODIS vertical profiles of atmospheric parameters include temperature and air moisture, given as dew point temperature, at 20 pressure levels, namely 1000, 950, 920, 850, 780, 700, 620, 500, 400, 300, 250, 200, 150, 100, 70, 50, 30, 20, 10, and 5 hPa. They are retrieved using a statistical regression procedure [13], often followed by a non-linear iterative physical algorithm [14], that uses clear sky radiances within a  $5 \times 5$  field of view (FOV) of approximately 5 km resolution over land and ocean both day and night. Processing is accomplished globally at  $5 \times 5$  pixel resolution in regions where a sufficient number of clear FOVs is available. Radiances within the clear FOVs are further averaged to reduce instrument single sample noise. The output product is released by the algorithm after all the input radiances passed a proper quality check; otherwise, the output product is labelled as missing. The factors that may affect the quality of retrievals are instruments noise, detector imbalances and spectral shifts. Many of these effects are difficult to characterize and correct. A complete error analysis includes the effects of ancillary input data errors. The retrieval algorithm requires calibrated 1 km radiances from bands 24 and 25 ( $4.46$  and  $4.52\ \mu\text{m}$ ) to estimate temperature profile, and bands 27, 28 and 29 ( $6.72$  to  $8.55\ \mu\text{m}$ ) for moisture profile. The MODIS Cloud Mask is used for cloud screening and for surface type determination (land or sea) [15, 16].

The MODIS/Terra platform overpasses the regions selected for this study twice a day. For the purpose of comparison with RS data, a preliminary analysis aimed at establishing the short-term variability of the atmospheric conditions was carried out. The ETA profiles were considered as reference data. In general, it resulted that smooth variations of the parameters relevant to this study occurred for the selected days. As a result, atmospheric stationary conditions were fulfilled for time lags not exceeding 3 hours. This interval was thus considered as the upper limit for time co-location of MODIS-RS profiles.

## 3. – Methodology

The three data sets herein considered resulted not homogeneous with respect to both space (horizontal and vertical) resolutions and acquisition times as well. Depending on the data set source, vertical sampling through the atmospheric column was available at different heights. In particular, ETA profiles were sampled with the highest resolution and MODIS profiles with the coarsest one. As a result, MODIS-RS profile comparison was carried out after reducing RS data to MODIS vertical resolution; besides, sampling rate of ETA profiles were reduced to RS vertical resolution. In both cases, sampling reduction was carried out using a simple averaging procedure in order to keep the statistical information content of the original data.

Geographic locations of MODIS profiles were selected at the corresponding RS site locations. Due to cloud coverage, MODIS profiles were extracted at the nearest geographic location of the corresponding RS station. As a result, the average horizontal distance between locations of MODIS profile and RS station was about 40 km with maximum separation of about 200 km. The nearest grid point was selected for the ETA profiles.

The maximum sampled height of RS data set is about 30000 m for Pratica di Mare station and 23000 m for Ajaccio station. ETA profiles extend from the first ETA level in air up to about 25000 m, the thickness of the layers being slowly increasing with the height and the vertical resolution decreasing with height. Therefore, it was chosen to analyze the temperature datasets up to 22000 m in the range from 1000 to 50 hPa, which includes about 16 vertical levels for RS-MODIS comparison and 30 vertical levels for RS-ETA comparison. Besides, moisture profiles were analyzed in the range from 1000 to 400 hPa, the highest (7000 m) corresponding to the maximum available height of the RS and MODIS datasets. As a result, moisture profiles include about 9 vertical levels for RS-MODIS comparison and about 20 vertical levels for RS-ETA comparison, respectively.

The RS-MODIS comparison is subjected to a temporal bias ranging from 45 minutes to 3 hours due to obvious lack of correspondence between satellite passage and RS acquisition times. It does not happen for the RS-ETA comparison because ETA simulations are available every hour.

We have chosen to perform the analysis on the following meteorological variables: temperature  $T$  (K), potential temperature  $\theta$  (K), dew point temperature  $d$  (K) and mixing ratio  $m$  (g/kg).

As previously mentioned, the MODIS retrieval algorithm produces vertical profiles of temperature  $T$  and dew point temperature  $d$ . The potential temperature  $\theta$  and mixing ratio  $m$  can be estimated using the following relations:

$$(2) \quad \theta = T \times [1000/P]^\kappa,$$

$$(3) \quad m = \frac{R_d}{R_v} \times \frac{e}{P - e} \times 1000 = 621.97 \times \frac{e}{P - e},$$

where  $P$  (hPa) is the pressure,  $e$  (hPa) is the vapour pressure,  $R_d$  and  $R_v$  are the gas constants for dry air and water vapour, respectively, and  $k$  is the Poisson constant defined as  $k = R_d/c_p \approx 2/7$ ,  $c_p$  being the specific heat at constant pressure.

The mixing ratio can thus be computed provided the vapour pressure is known. The definition of dew point temperature provides the relation between the vapour pressure  $e$  and the saturation vapour pressure ( $e^*$ ) at temperature  $d$ :  $e = e^*(d)$ . Different formulations of saturation vapour pressure can be considered: expressions derived from the Clausius-Clapeyron equation and formulas, in part based on experimental data [17, 18].

In this paper, two expressions relating the dew point temperature to vapour pressure have been considered:

- 1) the Bolton expression [19] as a modification of Tetens' [20] formula:

$$(4) \quad e = e^*(d') = 6.112 \times \exp \left[ \frac{17.67d'}{d' + 243.5} \right],$$

where  $d'$  is the dew point temperature expressed in degrees Celsius, and

2) an expression derived from the Clausius-Clapeyron equation [17]:

$$(5) \quad \ln \frac{e}{6.11} = \ln \frac{e^*(d)}{6.11} = \frac{L_{v0} - (c_{pv} - c_l)T_0}{R_v} \left( \frac{1}{T_0} - \frac{1}{d} \right) + \frac{c_{pv} - c_l}{R_v} \ln \frac{d}{T_0},$$

where  $c_l$  and  $c_{pv}$  are the heat capacity of liquid water and water vapour at constant pressure, respectively;  $L_{v0}$  is the latent heat of vaporization at  $T_0 = 273.15$  K.

In order to check the degree of reliability of the saturation vapour pressure evaluation as given by eqs. (4) and (5), we compared the values of  $e^*$  with the reference values obtained in the range of air temperature from  $-80^\circ\text{C}$  to  $50^\circ\text{C}$  with  $1^\circ\text{C}$  intervals by using the latest version of Goff-Gratch equation [21]. It is only slightly different from the equation used to construct the World Meteorological Organization Meteorological Tables [22]. The results of this comparison are provided expressing the temperatures in degrees Celsius as has been done in refs. [18,19,22]. The maximum absolute relative error (in percent) of Bolton's formulation, defined as the absolute value of the predicted value minus the reference value divided by the reference value, is 0.516 at  $50^\circ\text{C}$ . Furthermore, the discrepancies are less than 0.4% throughout the range of temperature from  $-66^\circ\text{C}$  to  $46^\circ\text{C}$ .

Expression (5) is resulted accurate to within 0.4% of values obtained from the Goff-Gratch equation in the range of temperature from  $-37^\circ\text{C}$  to  $50^\circ\text{C}$ .

Similar results were obtained after comparison of the saturation vapour pressure values from formulas (4) and (5) with those from the Goff-Gratch equation for temperatures below  $0^\circ\text{C}$  and Hyland and Wexler's equation [23] for temperature above  $0^\circ\text{C}$ , as recommended by Gueymard [22].

Figure 1a shows the mixing ratio profiles estimated by (4) and (5) formulations, and compared with the RS measurements for the case relevant to Ajaccio station gathered on the 19th of April 2000, 12:00 UTC.

The prognostic variables of the ETA model are temperature  $T$  and specific humidity ( $q$ ). While the potential temperature is computed using (2), the mixing ratio is obtained from the following expression:

$$(6) \quad m = \frac{q}{1 - q} \times 1000.$$

Besides, the dew point temperature  $d$  was estimated by inversion of (4) and (5) using the following expression from the equations of state for vapour pressure computation:

$$(7) \quad e = \frac{qP}{R_d/R_v + q(1 - R_d/R_v)}.$$

The inversion of eq. (4) was estimated by Bolton (1980) to give values of  $d'$  accurate within  $0.03^\circ\text{C}$  for the range from  $-35^\circ\text{C}$  to  $35^\circ\text{C}$ . Inverting (4) and using the saturation vapour pressure values depending on temperature from the Goff-Gratch equation, we found that the differences between the temperature calculated by eq. (4) and that relative to Goff-Gratch saturation vapour pressure were within  $0.04^\circ\text{C}$  in the range from  $-80^\circ\text{C}$  to  $39^\circ\text{C}$ .

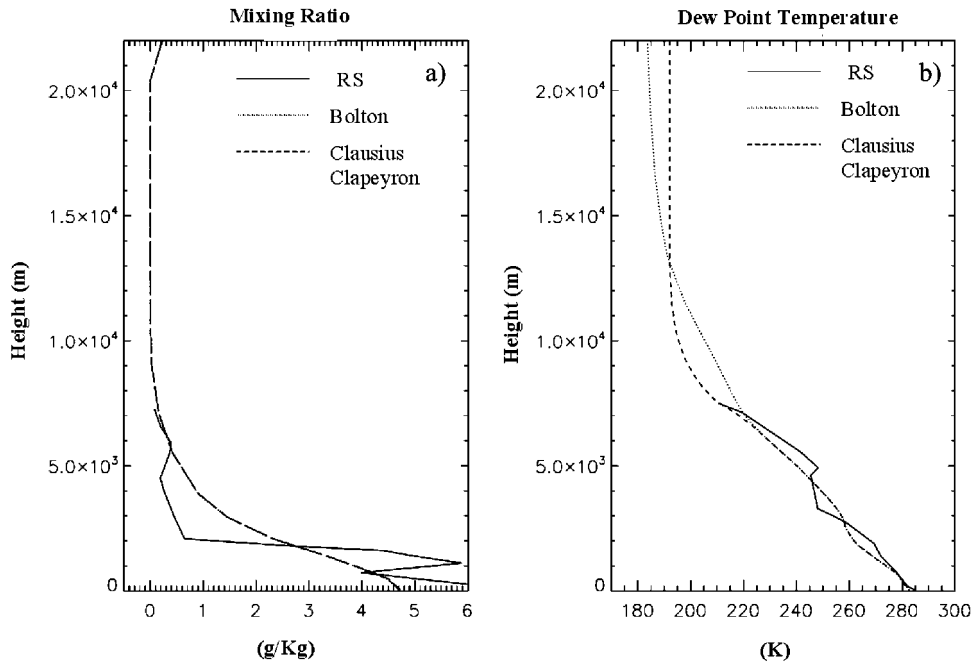


Fig. 1. – Ajaccio RS station: 19/04/2000, 12:00 UTC. MODIS mixing ratio  $m$  (a) and ETA dew point temperature  $d$  (b). Observed data: solid line; Bolton formula: dotted line; Clausius-Clapeyron formula: dashed line.

Figure 1b shows the comparison between the RS dew point temperature profile (solid line) and those calculated by ETA using Bolton (dotted line) and Clapeyron (dashed line) expressions, for the case relevant to Ajaccio station gathered on the 19th of April 2000, 12:00 UTC. The example reports the general behaviour found for all the analyzed data. For  $d$  values higher than about 220 K, to which there corresponds the range of heights where radiosonde data was available, there are only small differences between the two calculated dew point temperatures.

Alduchov and Eskridge [18], Elliot and Gaffen [24] analysed several formulations for  $e^*$  and found that the errors introduced by the use of different equations were negligible compared to the inherent inaccuracies of the sensors. With the aim of comparing RS, MODIS and simulated data, we found that expressions (4) and (5) were equivalent over most of the used temperature range.

Concerning the ETA profiles, the horizontal wind components  $u$  and  $v$  (m/s) were also available.

The vertical profiles of  $U$  and  $V$ ,  $T$ ,  $\theta$ ,  $d$  and  $m$ , measured at Ajaccio and Pratica di Mare RS stations, were compared to the same quantities simulated by ETA and obtained by MODIS. The following statistical indexes were computed to quantify the goodness of the evaluations: Fractional Bias (FB), Root Mean Square Error (RMSE) and Root Mean

Square Vector Error (RMSVE), defined as follows:

$$\begin{aligned}
 \text{FB} &= 2 \frac{\bar{x}_O - \bar{x}_P}{\bar{x}_O + \bar{x}_P}, \\
 \text{RMSE} &= \sqrt{\frac{1}{N} \sum (x_O - x_P)^2}, \\
 \text{RMSVE} &= \sqrt{\frac{1}{N} \sum [(U_O - U_P)^2 + (V_O - V_P)^2]},
 \end{aligned}
 \tag{8}$$

where the “*O*” subscript refers to the observed value by RS of the variable  $x$  and “*P*” refers to the retrieved one by MODIS or predicted one by ETA. RMSE is used to compare the scalar quantities (temperature, potential temperature, dew point temperature and mixing ratio), whereas RMSVE is used for wind components analysis.

The statistical analysis was performed also dividing the altitude range in six sub-ranges. To have a large set of data, for each sub-range we considered all the two sites together and all the different hours available. To complete the statistics, we also estimated the cumulative frequency distributions and the linear fit for all the corresponding couples of data.

#### 4. – Results and discussion

Data from two coastal RS stations were analyzed: Ajaccio (41.91° N, 8.80° E), Corsica (France) and Pratica di Mare (41.65° N, 12.43° E), Italy, for the days from 29th to 31st March 2000 and from 17th to 19th April 2000. The scheduled RS observations were every twelve hours at 00:00 UTC and 12:00 UTC for Ajaccio station, while every six hours from 00:00 UTC at Pratica di Mare station.

Figures 2-5 show the comparison between the observed variables profiles (solid line) and those simulated by ETA (dotted line) and retrieved by MODIS (dashed line). They refer to 12:00 UTC of 29 March at Ajaccio and 12:00 UTC of 30 March at Pratica di Mare. These figures are representative of the behaviour noticed in all the analyzed cases. In general, the shape of observed profiles is correctly reproduced by both ETA and MODIS results. Typically, temperature and potential temperature profiles compare well with observations; almost the same can be said for the dew point temperature, mixing ratio profiles and wind component profiles. Some differences are displayed in wind component profiles, in particular for Pratica di Mare station.

Although the overall shape is correctly reproduced, the strong fluctuations resulted highly smoothed. The latter result was indeed expected owing to the smoothed nature of both ETA and MODIS data. In fact, ETA predictions result from modelling procedure and MODIS outputs are relevant to volume averages. Both refer to mean quantities, while the corresponding observations are instantaneous and single-point values. Moreover, it should be taken into account the stochastic nature of the observed meteorological variables and the intrinsic errors of measurement of the instrumentation [25].

**4.1. ETA-RS comparison.** – The statistical indexes from RS data and ETA simulations are reported in table I for Ajaccio station and table II for Pratica di Mare station, respectively. They are relevant to 10 profiles (5 in March and 5 in April) for Ajaccio and to 17 profiles (8 in March and 9 in April) for Pratica di Mare. The results can be summarized as follows:



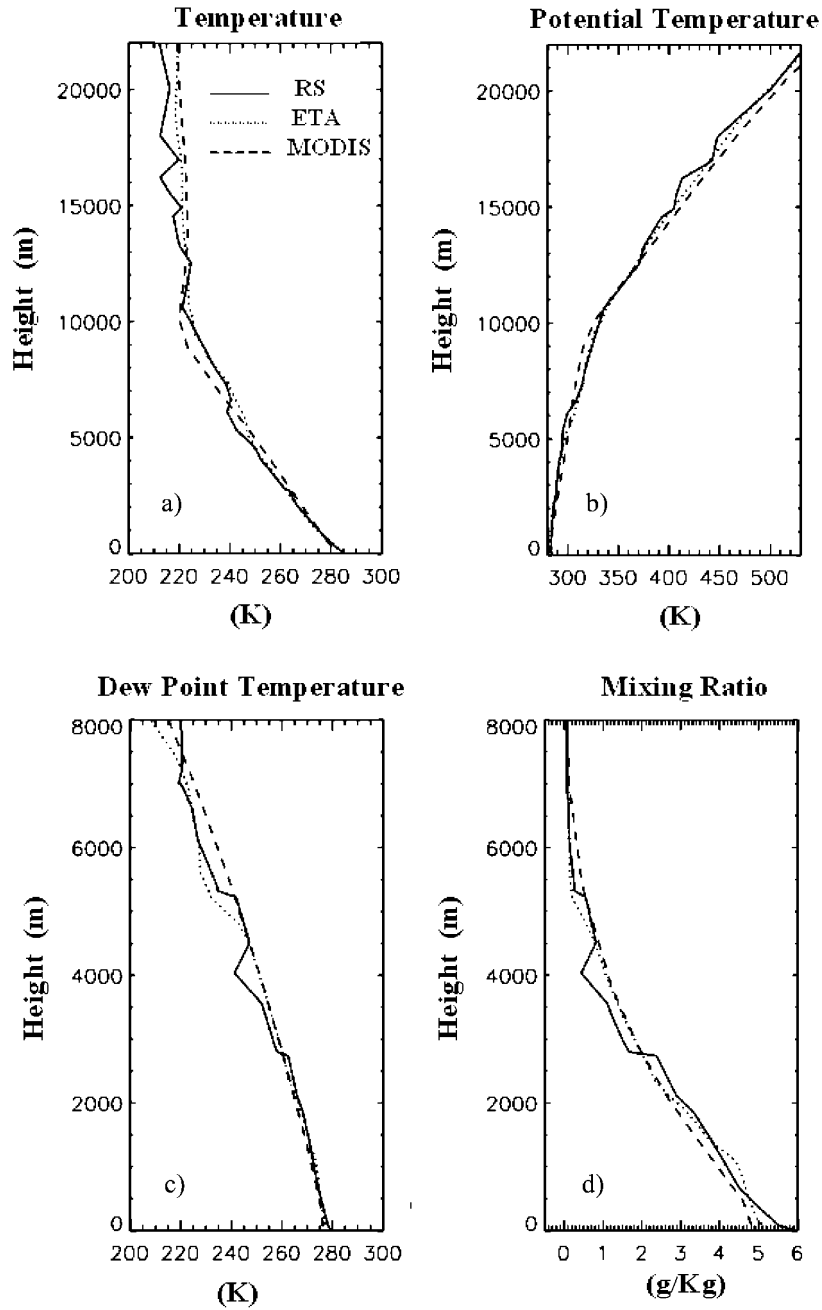


Fig. 2. – Ajaccio RS station: 29/03/2000, 12:00 UTC. Temperature  $t$  (a), potential temperature  $\theta$  (b), dew point temperature  $d$  (c) and mixing ratio  $m$  (d). Observed data: solid line; ETA: dotted line; MODIS: dashed line.

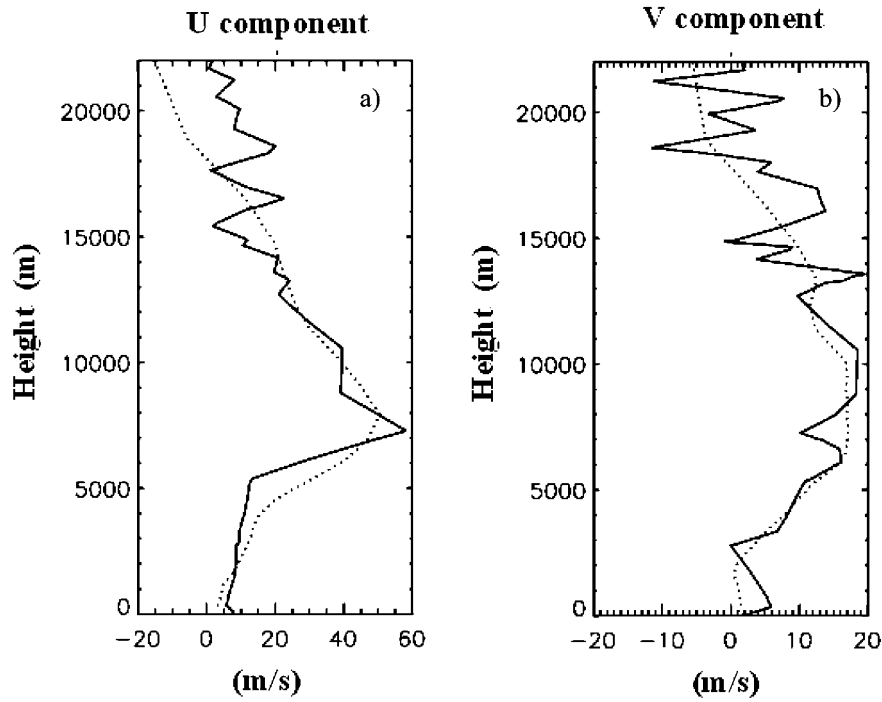


Fig. 3. – Ajaccio RS station: 29/03/2000, 12:00 UTC. Wind velocity components  $U$  (a) and  $V$  (b). Observed data: solid line; ETA: dotted line.

TABLE I. – *ETA: Ajaccio RS station, statistical indexes computed by considering all profiles.*

Ajaccio	Temperature (K)	Potential temperature (K)	Dew point temperature (K)	Mixing ratio (g/kg)	Wind (m/s)
RMSE	2.0	3.0	6.3	0.9	RMSVE 4.9
FB	-0.0018	-0.001	-0.003	-0.012	FB 0.098

TABLE II. – *ETA: Pratica di Mare RS station, statistical indexes computed by considering all profiles.*

Pratica di Mare	Temperature (K)	Potential temperature (K)	Dew point temperature (K)	Mixing ratio (g/kg)	Wind (m/s)
RMSE	2.0	3.0	8.3	1.4	RMSVE 6.0
FB	0.0006	-0.0017	-0.0016	-0.108	FB 0.059

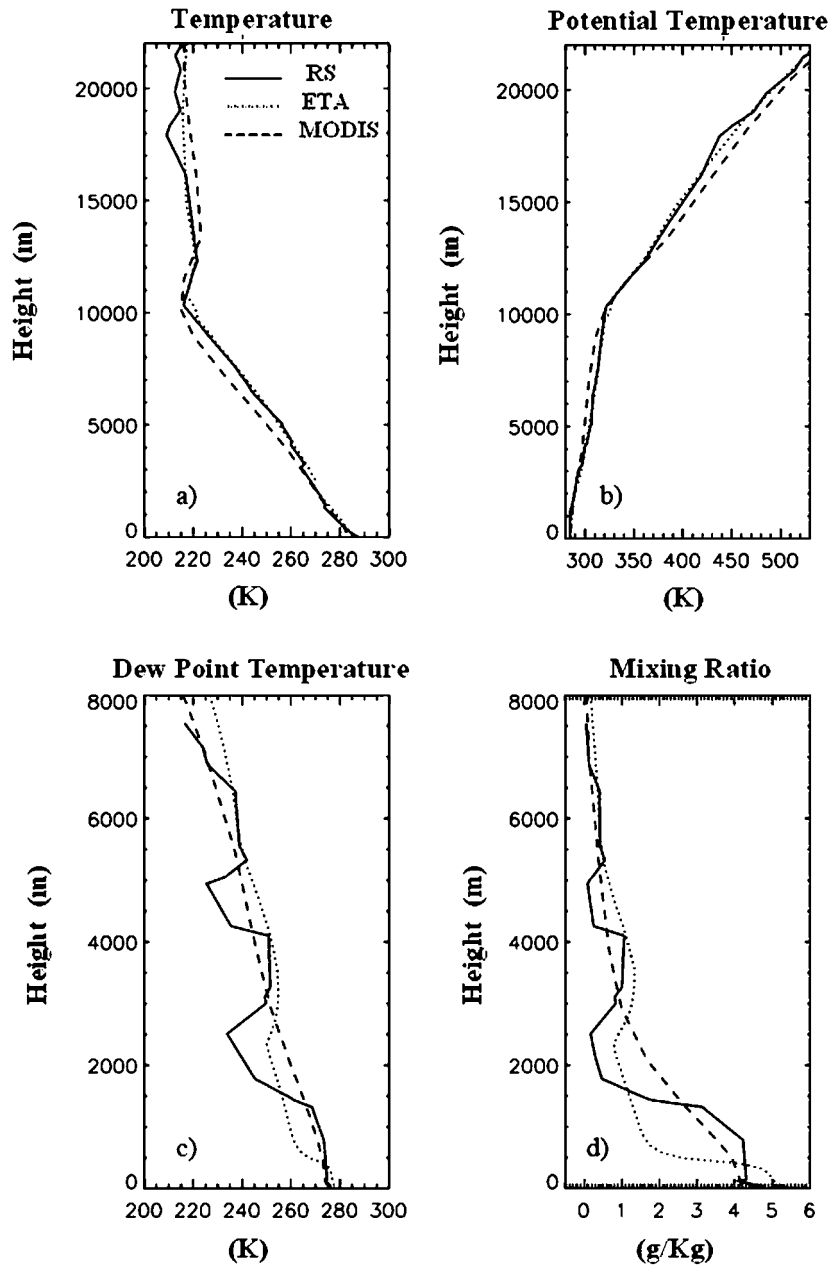


Fig. 4. – Pratica di Mare RS station: 30/03/2000, 12:00 UTC. Temperature  $t$  (a), potential temperature  $\theta$  (b), dew point temperature  $d$  (c) and mixing ratio  $m$  (d). Observed data: solid line; ETA: dotted line; MODIS: dashed line.

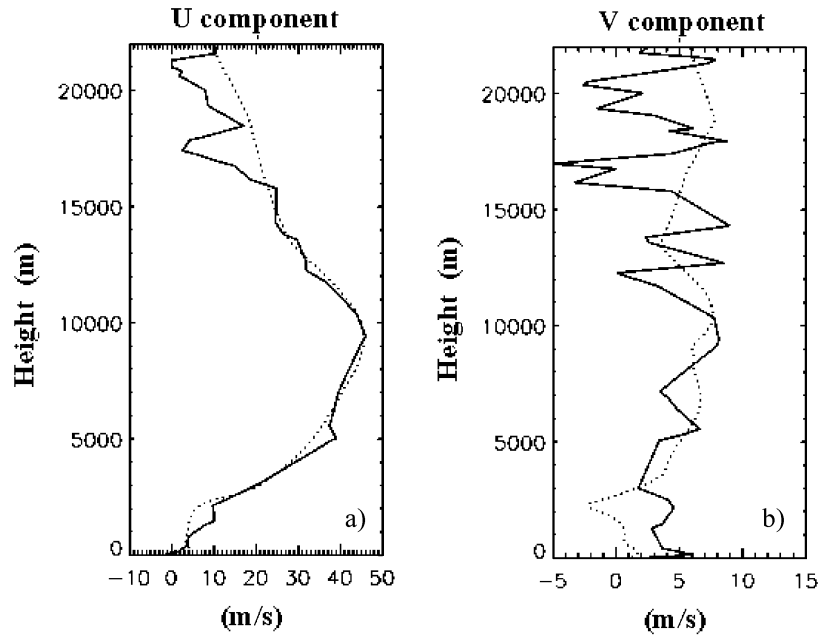


Fig. 5. – Pratica di Mare RS station: 30/03/2000, 12:00 UTC. Wind velocity components  $U$  (a) and  $V$  (b). Observed data: solid line; ETA: dotted line.

- Concerning dew point temperature, mixing ratio and wind velocity, RMSE resulted lower at Ajaccio than at Pratica di Mare. The same RMSE has been found for temperature and potential temperature.
- Fractional bias (FB) of potential temperature, dew point temperature and mixing ratio are negative for both the stations, thus showing ETA tendency to slightly overestimate these quantities.
- Positive FB's relevant to wind velocity occur for both stations. It can be deduced that ETA shows a tendency to slightly underestimate that quantity.
- FB of temperature does not show a systematic bias, being very close to zero at Pratica di Mare station and having opposite signs for the two stations.

The cumulative frequency distributions (c.f.d.) of temperature, potential temperature, dew point temperature and mixing ratio for ETA are compared with RS data in fig. 6. All the couples of ETA data with the corresponding RS observations for both stations were included. In general, ETA correctly reproduces the cfd of RS data, but slightly overestimates the lower temperature values and slightly underestimates the central values of the mixing ratio (fig. 6d).

In fig. 7 the cfd of wind velocity components,  $U$  (a) and  $V$  (b), are drawn. The agreement between ETA model and RS measurements is good and only minor differences can be seen. ETA overestimates slightly the negative values of the  $u$  component and slightly underestimates the  $v$  component.

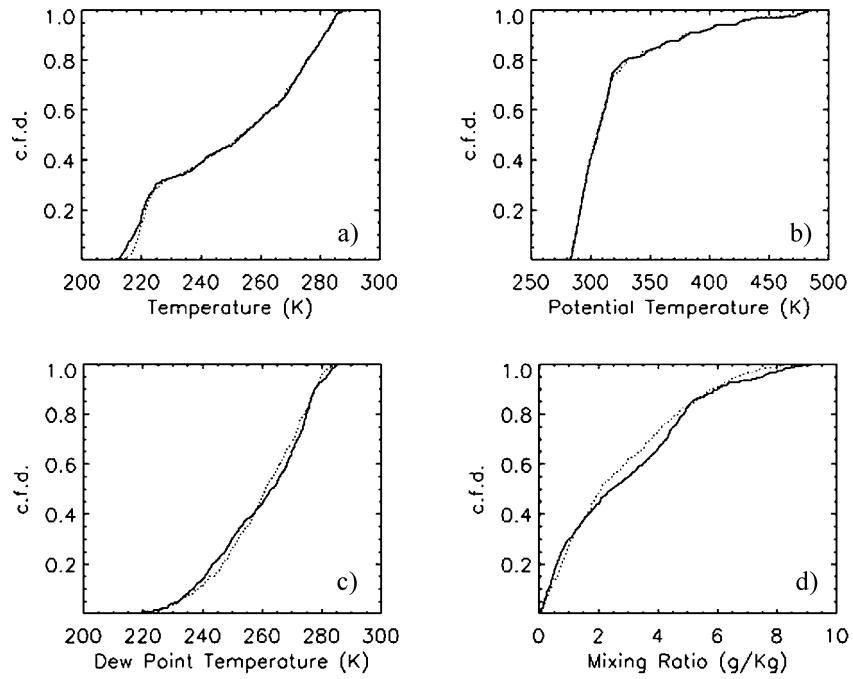


Fig. 6. – Cumulative frequency distributions (c.f.d.) of RS (solid line) and ETA data (dashed line) for the two RS stations Ajaccio and Pratica di Mare relevant to temperature (a), potential temperature (b), dew point temperature (c) and mixing ratio (d).

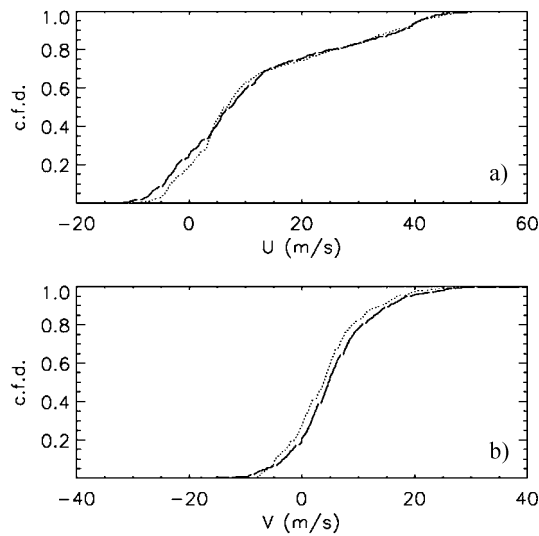


Fig. 7. – Cumulative frequency distribution of the data for Ajaccio and Pratica di Mare. Wind velocity components,  $U$  (a) and  $V$  (b). RS data: Solid line; ETA: dotted line.

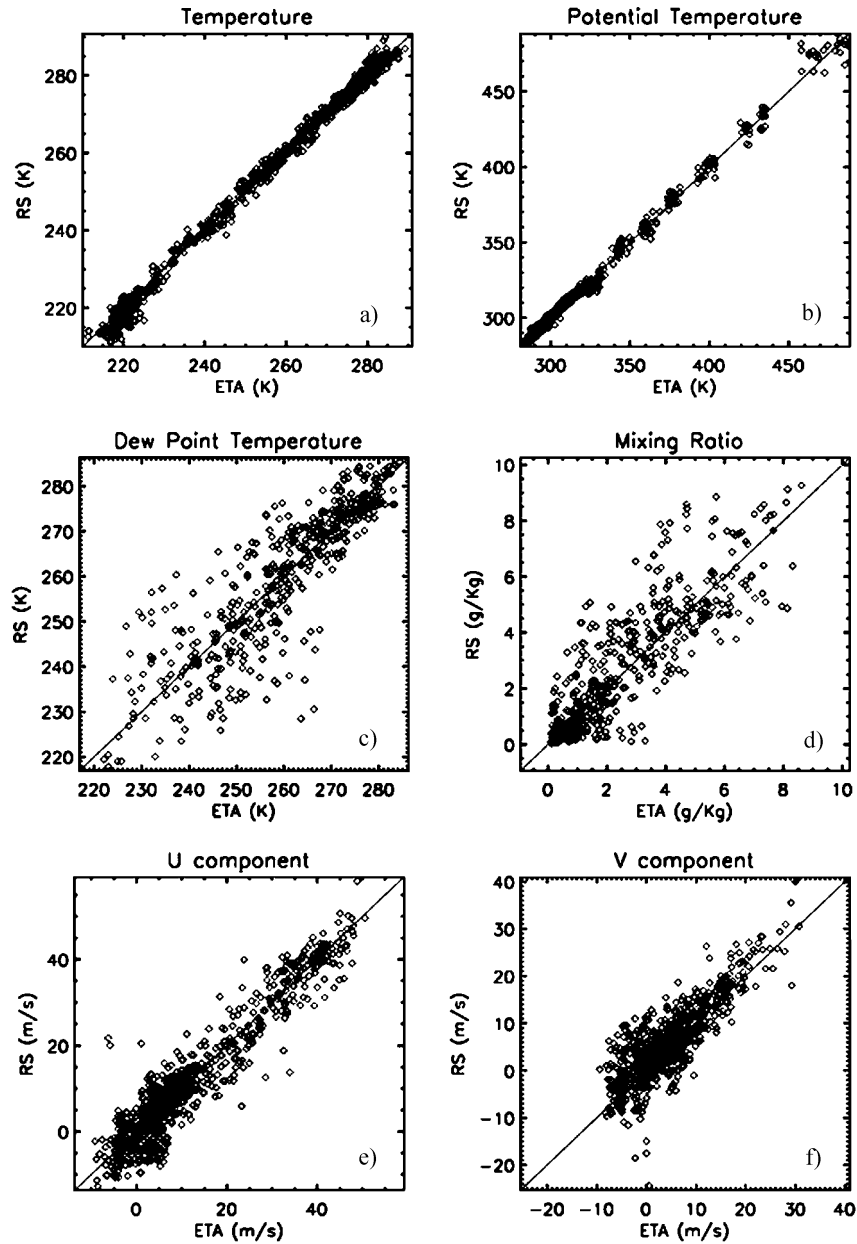


Fig. 8. – ETA: scatterplot of temperature (a), potential temperature (b), dew point temperature (c), mixing ratio (d) and wind velocity components,  $U$  (e) and  $V$  (f).

TABLE III. – *ETA: linear fit parameters for all the variables considered.*

ETA-RS	$b$	$c$	$r^2$
Temperature	$-5.9 \pm 0.7$	$1.022 \pm 0.003$	0.994
Potential temperature	$-1.5 \pm 0.8$	$1.005 \pm 0.002$	0.995
Dew point temperature	$13.0 \pm 6.5$	$0.950 \pm 0.025$	0.755
Mixing ratio	$0.4 \pm 0.1$	$0.932 \pm 0.026$	0.725
$U$ component	$-0.3 \pm 0.2$	$0.986 \pm 0.012$	0.898
$V$ component	$1.6 \pm 0.2$	$0.909 \pm 0.022$	0.690

The same procedure adopted to estimate cfd's was applied to compute linear regression of the parameters. Table III shows the intercept ( $b$ ), the slope ( $c$ ) and the squared linear correlation coefficient ( $r^2$ ). The analysis shows a good correlation for all the variable considered and in particular for temperature and potential temperature.

Finally, fig. 8 shows the scatter plots of all the variables considered for ETA.

**4.2. MODIS-RS comparison.** – Tables IV and V show the results of RS and MODIS comparisons: 9 profiles (5 in March and 4 in April) were available for Ajaccio RS station and 6 profiles (4 in March and 2 in April) for Pratica di Mare RS station. Although an higher number of RS acquisitions were available, either cloud coverage or temporal delay higher than 3 hours between MODIS passage and RS acquisition limited the use of corresponding MODIS imagery. The following conclusions can be drawn:

- For all the quantities, RMSE value is systematically higher for Pratica di Mare station than the Ajaccio one.
- In general, temperature, potential temperature and mixing ratio are underestimated by MODIS; besides, dew point temperature does not show any meaningful trend, as a result of the FB value that has opposite signs for the two stations.

From cross-comparison of the results obtained for ETA and MODIS, it can be observed that both statistical indexes for ETA are smaller than those corresponding to MODIS for the quantities, but the dew point temperature and the mixing ratio in Pratica di Mare, for which an higher RMSE has been estimated.

In fig. 9 the cumulative frequency distributions (c.f.d.) for MODIS are compared with RS data including both stations. In general, it should be pointed out that MODIS performs worse than ETA. A slight underestimation of the retrieved temperatures at

 TABLE IV. – *MODIS: Ajaccio RS station, statistical indexes computed by considering all profiles.*

Ajaccio	Temperature (K)	Potential temperature (K)	Dew point temperature (K)	Mixing ratio (g/kg)
RMSE	2.9	4.8	7.1	0.9
FB	0.004	0.003	-0.0011	0.068

TABLE V. – MODIS: Pratica di Mare RS station, statistical indexes computed by considering all profiles.

Pratica di Mare	Temperature (K)	Potential temperature (K)	Dew point temperature (K)	Mixing ratio (g/kg)
RMSE	4.3	6.0	7.9	1.1
FB	0.007	0.005	0.003	0.022

higher values (fig. 9a) has been observed. In contrast, it resulted a good agreement over almost all the interval of the potential temperatures (fig. 9b). For dew point temperature, MODIS slightly overestimates the values less than 260 K and underestimates higher temperatures (fig. 9c). In contrast, the cfd trend of mixing ratio is poor for values greater than about 3.0 g/kg (fig. 9d).

Table VI shows the intercept ( $b$ ), the slope ( $c$ ) and the squared linear correlation coefficient ( $r^2$ ) obtained considering MODIS data. As shown for ETA data, in this case a good correlation has been observed, especially for temperature and potential temperature. Besides, it can be noticed that ETA performs better than MODIS for temperature and potential temperature while MODIS shows a higher correlation coefficient than ETA if dew point temperature and mixing ratio are considered. In fig. 10 the scatter plots of all the variables considered are shown.

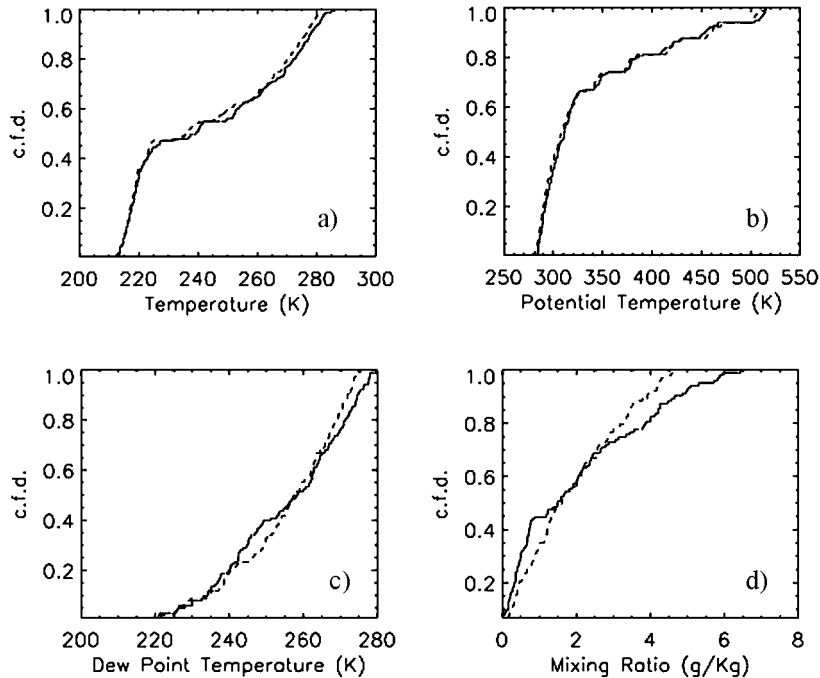


Fig. 9. – Cumulative frequency distributions (c.f.d.) of RS (solid line) and MODIS data (dashed line) for the two RS stations Ajaccio and Pratica di Mare relevant to temperature (a), potential temperature (b), dew point temperature (c) and mixing ratio (d).



TABLE VI. – MODIS: linear fit parameters for all the variables considered.

MODIS-RS	$b$	$c$	$r^2$
Temperature	$-3.8 \pm 2.2$	$1.021 \pm 0.009$	0.983
Potential temperature	$26.9 \pm 4.3$	$0.911 \pm 0.012$	0.964
Dew point temperature	$10.2 \pm 12.8$	$0.961 \pm 0.050$	0.784
Mixing ratio	$-0.2 \pm 0.2$	$1.150 \pm 0.069$	0.858

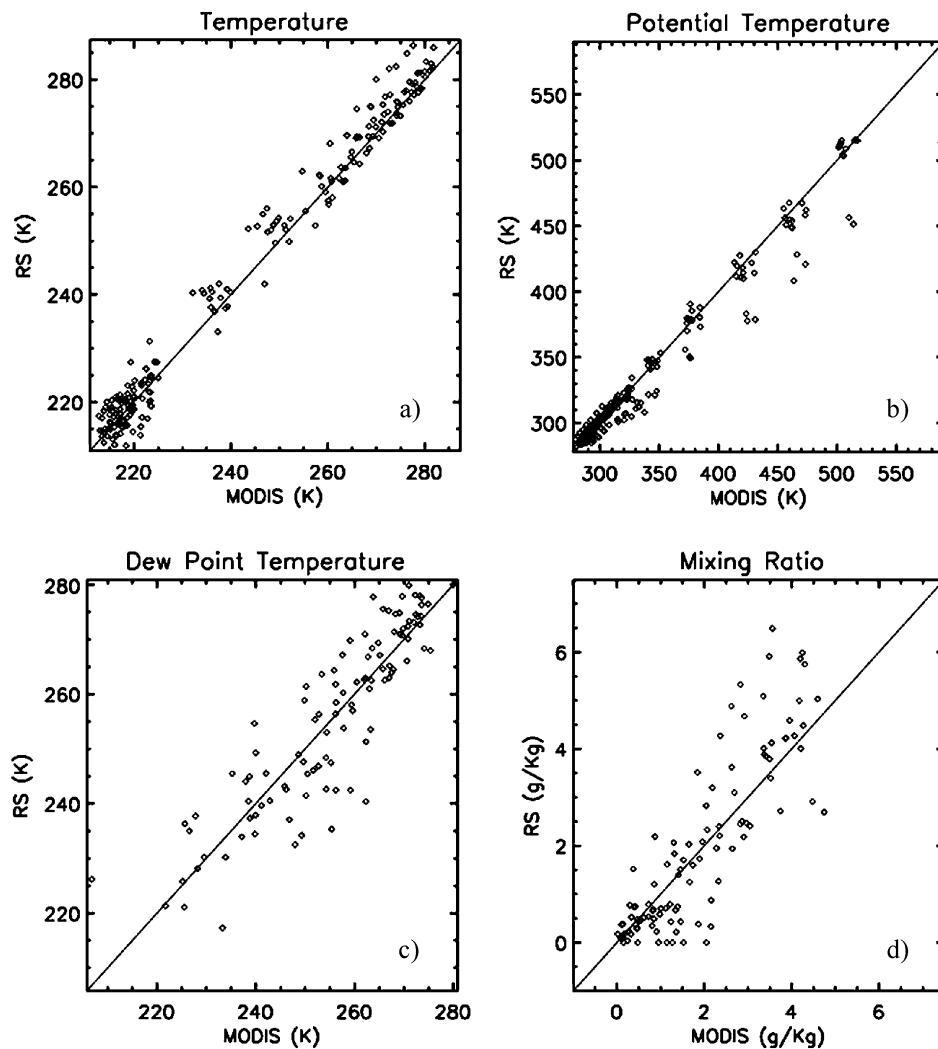


Fig. 10. – MODIS: scatterplot of (a) temperature, (b) potential temperature, (c) dew point temperature and (d) mixing ratio.

TABLE VII. – *Temperature subrange statistics for both radiosounding stations.*

Temperature	ETA #	RMSE	FB	MODIS #	RMSE	FB
$z \leq 1000$	99	1.7	-0.00003	21	3.8	0.009
$1000 < z \leq 2000$	100	1.6	-0.0001	15	4.0	0.007
$2000 < z \leq 3000$	76	1.3	0.001	29	3.5	0.007
$3000 < z \leq 4000$	62	1.7	0.001	16	3.2	0.001
$4000 < z \leq 6000$	104	1.7	0.002	15	5.1	0.014
$6000 < z \leq 9000$	112	1.8	0.0006	23	4.3	0.012
$9000 < z \leq 12000$	124	2.5	-0.006	37	2.4	0.005
$12000 < z \leq 17000$	99	1.8	-0.004	29	3.1	-0.0003
$z > 17000$	23	4.6	-0.016	26	3.2	-0.004

4.3. *Height dependence of ETA and MODIS statistical indexes.* – To evaluate how the two models perform as a function of the height, tables VII through XI report the statistical indexes after all the profiles were grouped in nine vertical sub-ranges (six for dew point temperature and mixing ratio) for the totality of pairs ETA-RS and MODIS-RS herein considered. The number of pairs used for each vertical sub-range is also reported.

Temperature RMSE for ETA was within 2 K up to 9000 m and in the range 12000–17000 m, while larger values were observed for MODIS. The same can be said for the potential temperature. The best value of temperature RMSE resulted between 2000–3000 m for ETA and between 9000–12000 m for MODIS (table VII). The best temperature FB for ETA resulted at heights less than 1000 m, while MODIS retrieved the best FB in the range 12000–17000 m. ETA potential temperature RMSE still has its best value in the

TABLE VIII. – *Potential temperature subrange statistics for both radiosounding stations.*

Potential temperature	ETA #	RMSE	FB	MODIS #	RMSE	FB
$z \leq 1000$	99	1.7	-0.000002	21	4.1	0.008
$1000 < z \leq 2000$	100	1.6	0.0001	15	4.6	0.008
$2000 < z \leq 3000$	76	1.4	0.002	29	4.5	0.007
$3000 < z \leq 4000$	62	1.7	0.0009	16	5.1	0.011
$4000 < z \leq 6000$	104	1.7	0.002	15	7.1	0.010
$6000 < z \leq 9000$	112	1.6	0.0015	23	8.9	0.017
$9000 < z \leq 12000$	124	3.9	-0.003	37	6.0	0.006
$12000 < z \leq 17000$	99	4.2	0.001	29	12.1	0.005
$z > 17000$	23	9.6	0.006	26	14.3	0.005

TABLE IX. – *Dew point temperature subrange statistics for both radiosounding stations.*

Dew point temperature	ETA #	RMSE	FB	MODIS #	RMSE	FB
$z \leq 1000$	99	5.3	0.007	21	5.6	0.010
$1000 < z \leq 2000$	100	5.9	0.002	15	4.8	0.007
$2000 < z \leq 3000$	76	8.4	-0.007	29	9.1	-0.009
$3000 < z \leq 4000$	62	11.2	-0.010	16	8.2	-0.001
$4000 < z \leq 6000$	104	9.8	0.003	15	7.4	0.006
$z > 6000$	34	5.8	-0.003	7	8.2	0.015

 TABLE X. – *Mixing ratio subrange statistics for both radiosounding stations.*

Mixing ratio	ETA #	RMSE	FB	MODIS #	RMSE	FB
$z \leq 1000$	99	1.8	0.122	21	2.5	0.522
$1000 < z \leq 2000$	100	1.2	0.050	15	2.0	0.166
$2000 < z \leq 3000$	76	1.2	0.008	29	2.1	-0.532
$3000 < z \leq 4000$	62	1.2	-0.008	16	2.3	-1.077
$4000 < z \leq 6000$	104	0.6	0.059	15	2.4	-1.418
$z > 6000$	34	0.2	-0.023	7	3.1	-1.821

 TABLE XI. – *Wind velocity subrange statistics for both radiosounding stations.*

Wind	ETA #	RMSVE	FB
$z \leq 1000$	99	7.9	-0.359
$1000 < z \leq 2000$	100	6.0	0.268
$2000 < z \leq 3000$	76	6.0	0.562
$3000 < z \leq 4000$	62	6.3	0.914
$4000 < z \leq 6000$	104	5.9	0.629
$6000 < z \leq 9000$	112	6.1	0.163
$9000 < z \leq 12000$	124	5.7	-0.202
$12000 < z \leq 17000$	99	7.0	-0.388
$z > 17000$	23	10.9	-0.459

range 2000-3000 m, while the corresponding best FB is once again for heights less than 1000 m (table VIII). As far as MODIS potential temperature indexes are concerned, the best RMSE resulted for heights lower than 1000 m and the best FB above 12000 m. Concerning the RMSE of dew point temperature, ETA and MODIS values were generally comparable. ETA performs better up to 1000 m, while MODIS between 1000 m and 2000 m. FB approaches zero between 1000 and 2000 m for ETA predictions and between 3000 and 4000 m for MODIS retrievals (table IX). In table X are listed the vertical behaviours of RMSE and FB for mixing ratio. The best value of RMSE resulted above 6000 m for ETA and between 1000 m and 2000 m for MODIS; the best ETA and MODIS FB are respectively in the range 2000-4000 m and 1000-2000 m.

As far as comparison of ETA wind velocity predictions as a function of height is concerned, table XI reports the results. It can be seen that the best values of RMSVE resulted between 9000 m and 12000 m and the best FB between 6000 m and 9000 m.

## 5. – Conclusions

The improvement of regional weather and climate model simulations is faced to the limited input observational information, especially in sparse and large areas such as oceans and polar regions. The capability to better characterize weather events is however hampered by the number of observations, although the conventional observation stations deployed in populated areas. There is thus a great interest to the exploitation of remotely sensed satellite observations.

In this work the results of a statistical comparison between the limited area model ETA [26], and the MODIS retrieval algorithm [15] against radiosoundings in the Tyrrhenian Sea are presented. Data from two coastal stations (Ajaccio, France and Pratica di Mare, Italy) were analysed for the periods from 29th to 31st March 2000 and from 17th to 19th April 2000. The smooth and slow variations of the atmospheric conditions that occurred during the selected days allowed comparison between MODIS and RS profiles with a temporal lag up to about three hours. An assessment of the goodness of the atmospheric profiles relevant to temperature, potential temperature, dew point temperature and mixing ratio was achieved. In particular, the approximate observational error of the MODIS data for each of considered variables was assessed. For the sake of completeness, the simulated ETA wind profiles were also presented. As general results, the mean variable profiles were reproduced with a satisfactory degree of reliability from both MODIS procedure and ETA model. However, as expected, they did not catch the largest fluctuations of the variables, likely due to the averaging on grid resolution inadequate to describe the smallest spatial scales. To quantify the comparisons, the statistical indexes Root Mean Square Error (RMSE) and Fractional Bias (FB) were considered. As a result, the statistical indexes relevant to temperature and potential temperature for ETA simulations turned out better than the corresponding ones of MODIS retrievals, while they were of comparable quality (in some cases higher) for dew point temperature and mixing ratio.

Nevertheless, the most useful aspect of the MODIS atmospheric profiles relies on the daily global coverage with 5 km horizontal resolution at nadir. As a proof of concept, the results presented in this paper suggest that the MODIS retrieved profiles of temperature and water vapour, if exploited in assimilation schemes related to high-resolution weather models, could have a significant impact on the simulated variables, in particular for oceans and remote regions where conventional atmospheric soundings are lacking or even missing.

\* \* \*

We acknowledge that MODIS data used for this study were freely downloaded from the distribution site <http://daac.gsfc.nasa.gov/data/dataset/> and radiosoundings were retrieved from the archive of the University of Wyoming (<http://weather.uwyo.edu/upperair/sounding.html>) The authors would also acknowledge the three anonymous reviewers for their valuable and constructive comments.

## REFERENCES

- [1] <http://www.ua.nws.noaa.gov/factsheet.htm>.
- [2] ANDERSSON E., in *Polar Meteorology, Seminar Proceedings 4-8 September 2006, ECMWF, Shinfield Park, Reading, Berkshire RG2 9AX, UK, March 2007*, pp. 89-101.
- [3] MCNALLY T., in *Polar Meteorology, Seminar Proceedings 4-8 September 2006, ECMWF, Shinfield Park, Reading, Berkshire RG2 9AX, UK, March 2007*, pp. 103-114.
- [4] MESINGER F., *Riv. Meteorol. Aeronautica*, **44** (1984) 195.
- [5] MESINGER F. and JANJIC Z. I., in *Observation, theory and modelling of orographic effects, Seminar/Workshop 1986, ECMWF, Shinfield Park, Reading, Berkshire RG2 9AX, UK, 2*, (1987), pp. 29-80.
- [6] JANJIC Z. I., *Mon. Weather Rev.*, **122** (1994) 927.
- [7] GEORGELIN M., RICHARD E., PETITDIDIER M. and DRUILHET A., *Mon. Weather Rev.*, **122** (1994) 1509.
- [8] CHEN F., MITCHELL K., SCHAAKE J., XUE Y., PAN H. L., KOREN V., DUAN Q. Y., EK K. and BETTS A., *J. Geophys. Res.*, **101** (1996) 7251.
- [9] JANJIC Z. I., in *Research activities in atmospheric and oceanic modeling*, WMO Weather Prediction Research Programme, No. 23 (1996), pp. 4.14-4.15.
- [10] PAULSON C. A., *J. Appl. Meteorol.*, **9** (1970) 857.
- [11] LOBOCKI L., *J. Appl. Meteorol.*, **32** (1993) 126.
- [12] KING M. D., KAUFMAN Y. J., MENZEL W. P. and TANRE D., *IEEE Trans. Geosci. Remote Sensing*, **30** (1992) 2.
- [13] SMITH W. L., WOOLF H. M. and JACOB W. J., *Mon. Weather Rev.*, **8** (1970) 582.
- [14] LI J., WOLF W., MENZEL W. P., ZHANG W., HUANG H. L. and ACHTOR T. H., *J. Appl. Meteorol.*, **39** (2000) 1248.
- [15] MENZEL W. P., SEEMANN S. W., LI J. and GUMLEY L. E., in [http://modis-atmos.gsfc.nasa.gov/\\_docs/atbd\\_mod07.pdf](http://modis-atmos.gsfc.nasa.gov/_docs/atbd_mod07.pdf), ATBD-MOD-07, NASA Goddard Space Flight Center 2002.
- [16] KING M. D., MENZEL W. P., KAUFMAN Y. J., TANRE D., GAO B. C., PLATNICK S., ACKERMAN S. A., REMER L. A., PINCUS R. and HUBANKS P. A., *IEEE Trans. Geosci. Remote Sensing*, **41** (2003) 442.
- [17] EMANUEL K. A., in *Atmospheric Convection* (Oxford University Press, Oxford) 1994, pp. 116-117.
- [18] ALDUCHOV O. A. and ESKRIDGE R. E., *J. Appl. Meteorol.*, **35** (1996) 601.
- [19] BOLTON D., *Mon. Weather Rev.*, **108** (1980) 1046.
- [20] TETENS D., *Z. Geophys.*, **6** (1930) 297.
- [21] GOFF J. A., *Humidity and Moisture measurement and Control in Science and Industry*, Vol. **3**, edited by WEXLER A. and WILDHACK W. H. (Reinold Publ.) 1965, p. 289.
- [22] GUEYMARD C., *J. Appl. Meteorol.*, **32** (1993) 1294.
- [23] HYLAND R. W. and WEXLER A., *ASHRAE Trans.*, **89** (2A) (1983) 500.
- [24] ELLIOT W. P. and GAFFEN D. J., *Bull. Am. Meteorol. Soc.*, **72** (1991) 1507.
- [25] GREENE J. S., COOK W. E., KNAPP D. and HAINES P., *J. Atmos. Oceanic Technol.*, **19** (2002) 397.
- [26] MESINGER F., JANJIC Z. I., NICKOVIC S., GAVRILOV D. and DEAVEN D. G., *Mon. Weather Rev.*, **116** (1988) 1493.